Supporting Information

Fusion of amyloid beta with ferritin yields an isolated oligomeric beta-sheet-rich aggregate inside the ferritin cage

Basudev Maity,[1] Shiori Kameyama,[1] Jiaxin Tian,[1] Thuc Toan Pham,[1] Satoshi Abe,1 Eri Chatani,[2] Kazuyoshi Murata,[3,4] Takafumi Ueno,[1,5] *

[1]School of Life Science and Technology, Tokyo Institute of Technology, Nagatsuta-cho 4259, Midori-ku, Yokohama 226 8501, Japan.

[2] Department of Chemistry, Graduate School of Science, Kobe University, Kobe, Hyogo 657-8501, Japan

[3]Exploratory Research Center on Life and Living Systems (ExCELLS), National Institute for Natural Sciences, Okazaki, Aichi, 444-8585, Japan.

[4]National Institute for Physiological Sciences (NIPS), National Institute for Natural Sciences, Okazaki, Aichi, 444-8585, Japan

[5] Living Systems Materialogy (LiSM) Research Group, International Research Frontiers Initiative (IRFI), Tokyo Institute of Technology, Nagatsuta-cho 4259, Midori-ku, Yokohama 226-8501, Japan

Experimental section

Materials and physical methods

The chemicals used in this work were purchased from TCI, Wako etc. and used as received. The UV-visible spectra were measured on a UV-2400PC UV–vis spectrometer (Shimazu). The matrix-assisted laser desorption ionization time-of-flight mass spectrometry, MALDI-TOF-MS (Bruker ultrafle Xtreme) was used to determine the mass of the protein monomers.

Cloning and purification of Fr-Aβ42

Fusion construct of **Fr-Aβ42** was prepared by Gibson assembly method in which a linearized PMK2 vector containing the ferritin gene and an Aβ insert were used for fusion.[1] Thus prepared PMK2 vector containing **Fr-Aβ42** gene was transformed into NovaBlue competent cells (Novagen) for protein expression. The expression and purification of **Fr-Aβ42** was done using previously reported procedure with little modification.[2] *E. coli* pallet, 20 g in 50mM Tris-HCl (pH 8.0) was sonicated and cell debris were separated by centrifugation. Then, the supernatant containing **Fr-Aβ42** was heated to 70 °C with stirring for 15 min followed by cooling and centrifugation. The supernatant was then filtered and purified by anion exchange (Q-Sepharose) and size exclusion (S300) chromatography. Purity of the **Fr-Aβ42** was checked by native PAGE (7.5%). Protein concentration was determined using the molar extinction coefficients of 382325 $M^{-1}cm^{-1}$ (For **Fr-Aβ42**) and 346560 $M^{-1}cm^{-1}$ (FrWT), as obtained from https://web.expasy.org/protparam/.

Crystallization and X-ray structure determination

The **Fr-Aβ42** in 50 mM Tris-HCl (pH 8.0) /0.15 M NaCl was crystallized by hanging drop vapor diffusion method as described in our previous report.[3] Typically, the crystallization drops were prepared by mixing a 1:1 ratio of **Fr-Aβ42** (10-15 mg/ml) and the precipitant solution (0.5-1.0 M $(NH_4)_2SO_4$, 15-17 mM $CdSO_4$). *Caution*!!: The solution of $CdSO_4$ is hazardous and thus, proper

precaution should be taken while use. The crystallization drops were allowed to equilibrate against the 500 µL of precipitant solution at 20 °C. The crystals appeared after one day and allowed to grow further.

The X-Ray diffraction measurement was performed at 100K using Rigaku XtaLAB Synergy diffractometer (Cu K-alpha, λ = 1.542 Å). A single crystal of **Fr-Aβ42** was soaked into a cryoprotectant solution containing 1.0 M $(NH_4)_2SO_4$, 15 mM $CdSO_4$ and 25 % (v/v) ethylene glycol for 30 seconds and subsequently mounted on the goniometer for X-ray diffraction measurement. After measurement, the data were automatically processed with CrysAlis Pro software (v40). The data were merged and scaled in AIMLESS program in CCP4i. The structure of **Fr-AB42** was constructed by molecular replacement method (MOLREP in CCP4) in which a FrWT structure (pdb ID: 1DAT) was used as an initial model for phasing.[4] The **Fr-Aβ42** structure was refined using REFMAC5[5] in CCP4i and the model was rebuilded in COOT[6] based on the $2F_o$-F_c and F_o-F_c electron density maps. We assigned the waters molecules based on F_o-F_c density map (3σ) in COOT. The refinement and model building were continued until a reasonable structure of **Fr-AB42** was obtained. The final structure was validated by Molprobity.[7] The residues after 171 was not modelled due to lack of enough density. Selected crystallographic and refinement parameters are given in Table S4. Atomic coordinate of **Fr-Aβ42** is deposited in the Protein Data Bank (Code: 8KH2).

Transmission emission microscopy (TEM) Measurement

TEM measurements of FrWT or **Fr-Aβ42** were conducted in a JEOL 1400-Plus electron microscope (JEOL, Tokyo, 120 kV). An aliquot of 5 µl of FrWT or **Fr-Aβ**42 from a 400 nM stock in 50 mM Tris-HCl (pH 8.0)/0.15 M NaCl was placed on a carbon-coated copper grid and allowed to immobilize the protein for 1 minute. Then, the buffer was blotted away and the grid was washed

three times with Milli-Q water to remove any unimmobilized proteins. The sample immobilized on the grid was stained with 5 µL of 1% methyl-amine tungstate (Nanoprobes, CAS No. 55979-60-7) for 1 minute and blotted away after that. Finally, the protein Samples were imaged at 80kV in the electron microscope. For size distribution, over 100 ferritin particles (200x or 100x magnification) were manually picked and measured the diameter using ImageJ software.

ThT assay

ThT assay was carried out using Perkin Elmer Luminescence spectrometer. A mixture 1.0 µM protein (FrWT or **Fr-Aβ42**) and 10 µM ThT in 50 mM Tris-HCl, pH 8.0 containing 0.15 M NaCl was incubated at RT for 30 min and then the ThT fluorescence was recorded by setting the excitation wavelength at 440 nm. ThT fluorescence inhibition study was performed using the mixture of 1 µM of **Fr-Aβ42**, 10 µM of ThT and gallic acid (250 µM and 500 µM) in 50 mM Tris-HCl, pH 8.0 containing 0.15 M NaCl. The ThT fluorescence intensity at 480 nm was monitored in every 1h interval to see the inhibition effect. A control experiment without gallic acid was also done parallelly. Since gallic acid oxidation is faster in alkaline pH, we also performed a control experiment in a 50 mM K-Phos buffer (pH 6.8) /0.15 M NaCl (Figure S6).

Size exclusion chromatography was done in Hitachi LaChrom Elite HPLC System. The Shodex Asahipak GF-510 HQ column was used. A mixture of 0.5 µM protein (FrWT or **Fr-Aβ42**) and 25 µM ThT in 50 mM Tris-HCl (pH 8.0) / 0.15 M NaCl was incubated at RT for 2h and then the mixture was concentrated to about 11-14 µM (protein). The 20 µl of the concentrated protein mixture was injected for HPLC. The protein was eluted with 20 mM Tris-HCl (pH 8.0) with a flow rate 0.5 ml/min. Absorbance was set at 280 nm for protein and Excitation was set at 440 nm for ThT fluorescence.

ATR-IR Measurement

The ATR-IR measurements for FrWT and **Fr-Aβ42** samples were done using FT-IR4200 instrument (JASCO). A 5 μL of the ~50 μM of protein samples were placed on the IR sample probe and air dried and then measured the spectra. The number of scans was 32 and the resolution was $4cm^{-1}$. A background was measured without putting any sample.

Circular dichroism (CD) spectropolarimetry

CD spectra of FrWT and **Fr-Aβ42** were measured on the J-820 CD spectrometer (JASCO). A quartz cuvette with a path length of 0.1 cm was used. The FrWT and **Fr-Aβ42** samples with a concentration of 0.1 mg/ml in 50mM Tris-HCl, pH 8, 150mM NaCl, were used for the study. The CD spectra were recorded in the far-UV region with a wavelength range of 190–260 nm at 25°C, averaging three scans with a bandwidth of 1 nm. CD temperature scans for FrWT and **Fr-Aβ42** were performed at λ =222 nm, starting from 25°C to 99.5 °C, with a thermal gradient of 1 °C /min.

DLS measurement

DLS measurement was carried out in 50 mM Tris-HCl, pH 8.0 containing 0.15 M NaCl on a Malvern Zetasizer Nano ZSP with a temperature controller. Protein samples were filtered (0.2 μm) before measurement. Hydrodynamic diameters were obtained from volume percent distribution. Standard deviation of the DLS data were calculated from three independent experiment.

HS-AFM measurement

The HS-AFM (RIBM, Tsukuba, Japan) experiments were done similarly as in our previous reports.[8, 9] The amorphous carbon tip of about >100 nm length on the BL-AC10-DS-A2 cantilever (Olympus, Tokyo, Japan; k = 0.1 N/m, f = 400~500kHz in water) was grown by electron beam deposition method. A mica disc (diameter 1.5 nm) was fixed on the quartz glass cylinder which was previously fixed on the Z-scanner. 2 μl of the ferritin samples in 50mM Gly-HCl (pH 2.3) containing 100 mM

of KCl was placed on a freshly cleaved mica surface and allowed to adsorb on the mica surface for 5 min followed by rinsing of un-adsorbed protein with pH 2.3 buffer. Then the Z-scanner was placed over the cantilever which is immersed in the buffer solution. The HS-AFM measurement was performed in tapping mode.

Analysis of the HS-AFM images and the HS-AFM movies were prepared using IGOR Pro (WaveMetrics) based software developed at Nagoya University. The HS-AFM images if needed were processed by low-pass (2 nm) fast Fourier transform (FFT) frequency-filtering techniques. The time point 0 s in HS-AFM movies does not represent the absolute starting point of the process like disassembly or dynamic changes. This is the starting point of a selected movie clip from a continuous process.

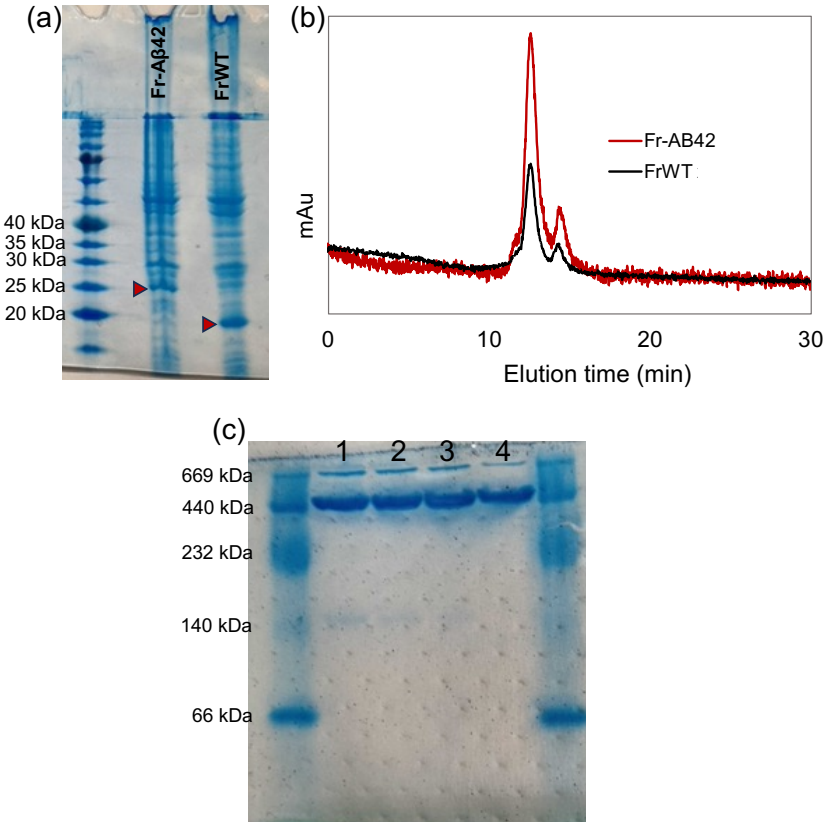

Figure S1. (a) Polyacrylamide SDS gel (12.5%) electrophoresis of *E. Coli* cells after sonication, showing the expression level of FrWT and **Fr-Aβ42**. Condition: 50 mg of *E. Coli* cells in 50 mM Tris-HCl (pH 8.0), followed by cell disruption using sonication. Thus obtained cell lysate was directly used for SDS PAGE. (b) Size exclusion chromatography shows the elution profile of FrWT and **Fr-Aβ42** in 20 mM Tris-HCl buffer (pH 8.0) containing 0.15 M NaCl. Flow rate: 0.5 ml /min. (c) Native polyacrylamide gel electrophoresis of FrWT and **Fr-Aβ42**. Lane 1: FrWT freshly prepared; lane 2: FrWT after 20 days at RT (25 °C); lane 3: **Fr-Aβ42** freshly prepared; lane 4: **Fr-Aβ42** after 20 days at RT (25 °C). The freshly prepared samples, which were stored at -80 °C, were allowed to equilibrate to room temperature and then used immediately for this native PAGE.

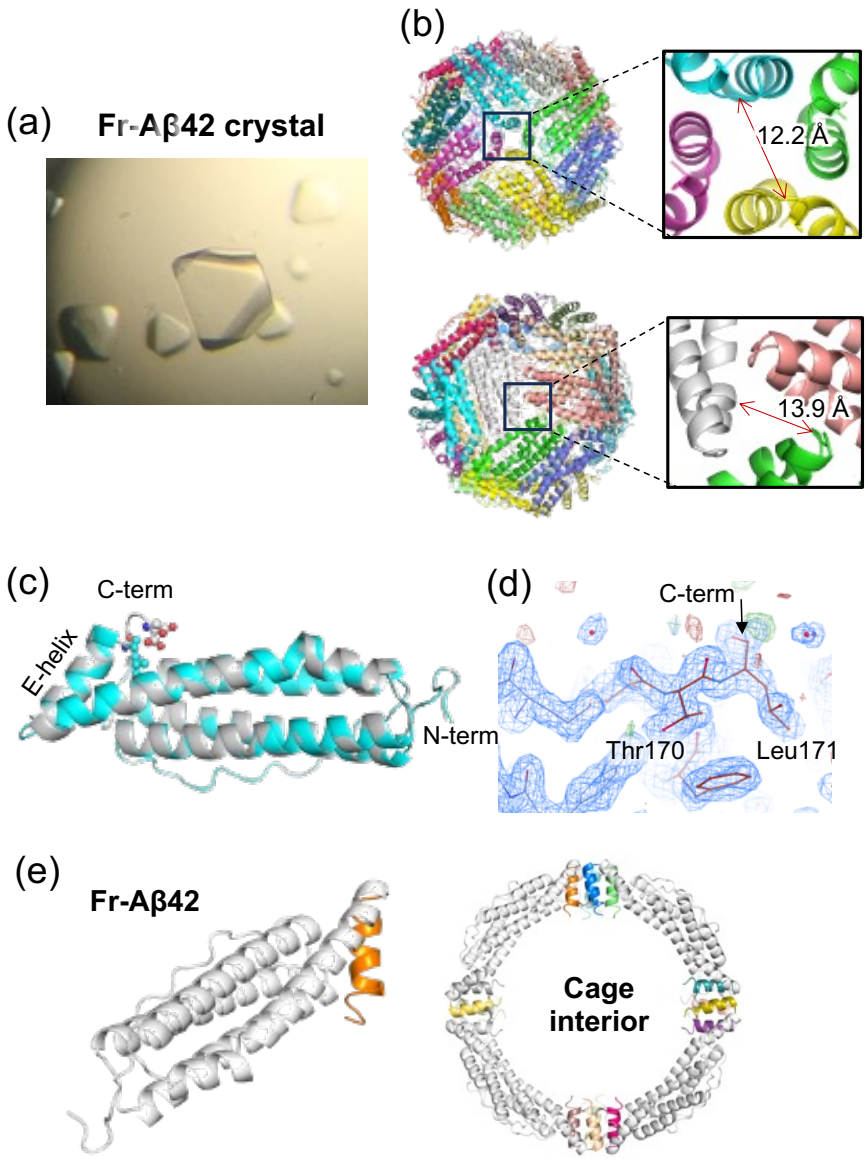

Figure S2. X-ray crystal structure analysis of **Fr-Aβ42**. (a) An optical image of the single crystals of **Fr-Aβ42**. The size of the larger crystal is around 400 μm. (b) X-ray crystal structure analysis (2.0 Å resolution) showing the 24-mer cage structure of **Fr-Aβ42** facing forward the 4-fold and 3-fold channel. Inset shows the expanded view of the channels with selected distance. (c) Superposition of the monomers of FrWT (grey) and **Fr-Aβ42** (cyan). The last residue (Asp174 for FrWT and Leu171 for **Fr-Aβ42**) is shown in sphere model. (d) $2F_o$-F_c electron density map (1σ) near the C-terminal of **Fr-Aβ42** showing the lack of density corresponding to the fused Aβ peptide. (e) A monomer structure of **Fr-Aβ42** and its location in the ferritin cage. The E-helices are colored. It is showing that the E-helices are located inside the cage, which means the fused Aβ peptides are located inside the cage but not modeled due to the lack of electron density.

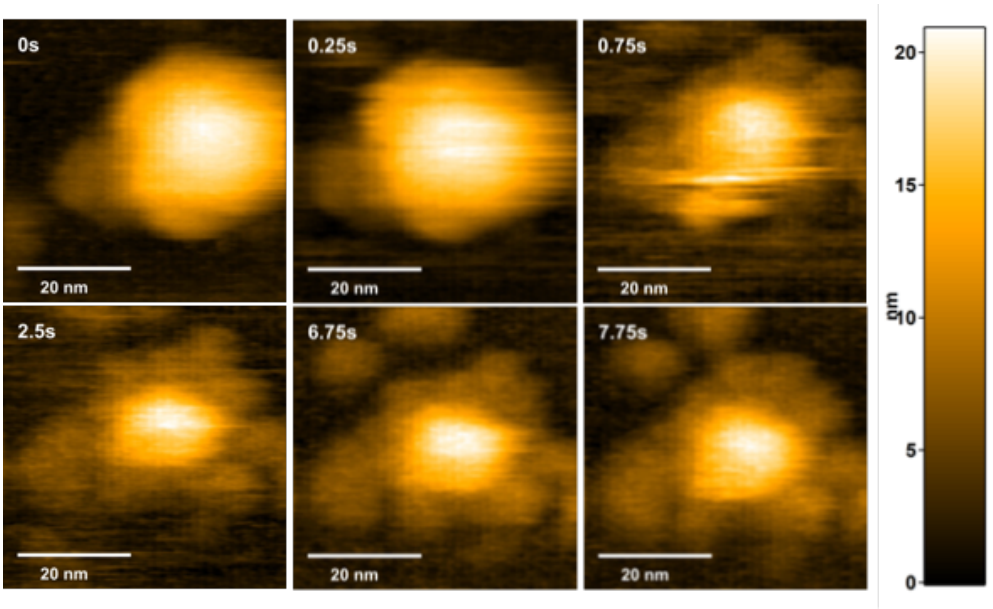

Figure S3: Selected HS-AFM snapshots of a single **Fr-Aβ42** cage disassembly and observation of the encapsulated AβO inside the cage. The measurement was conducted in a buffer solution at pH 2.3 (50 mM Gly-HCl /0.1 M KCl). The figure represents an additional observation of the single cage disassembly as described in Figure 3a. The snapshots are taken from original HS-AFM movie 2.

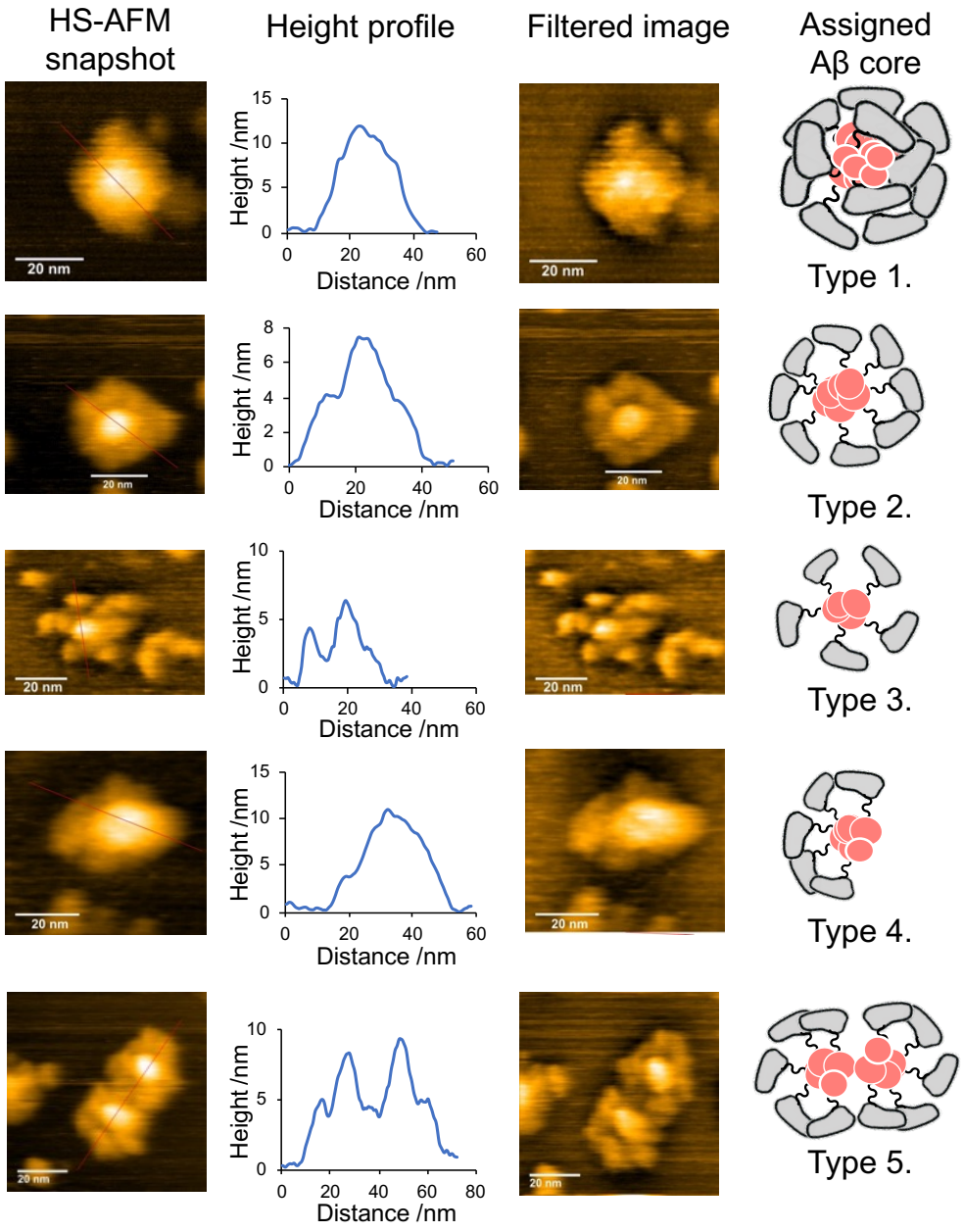

Figure S4: Various types of Aβ cores formed after the disassembly of **Fr-Aβ42** in pH 2.3 buffer (50 mM Gly-HCl /0.1M KCl). The filtered images were processed with a band pass filter (Low2 and High 40) for better vieweing of the amyloid core.

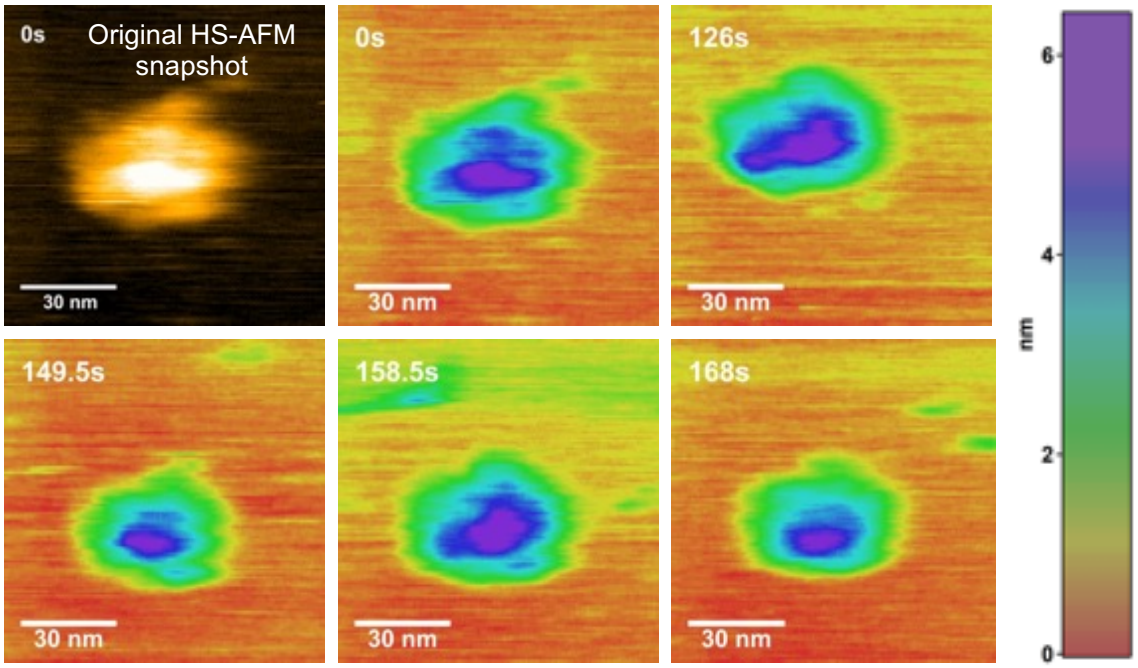

Figure S5: Heat-plot showing the time-dependent dynamic structural changes of an amyloid core overtime. The measurement was conducted in 50 mM Gly-HCl / 0.1 M KCl (pH 2.3). The figure represents an additional observation of the AβO dynamics with time, as described in Figure 3e. The snapshots are taken from original HS-AFM movie 5.

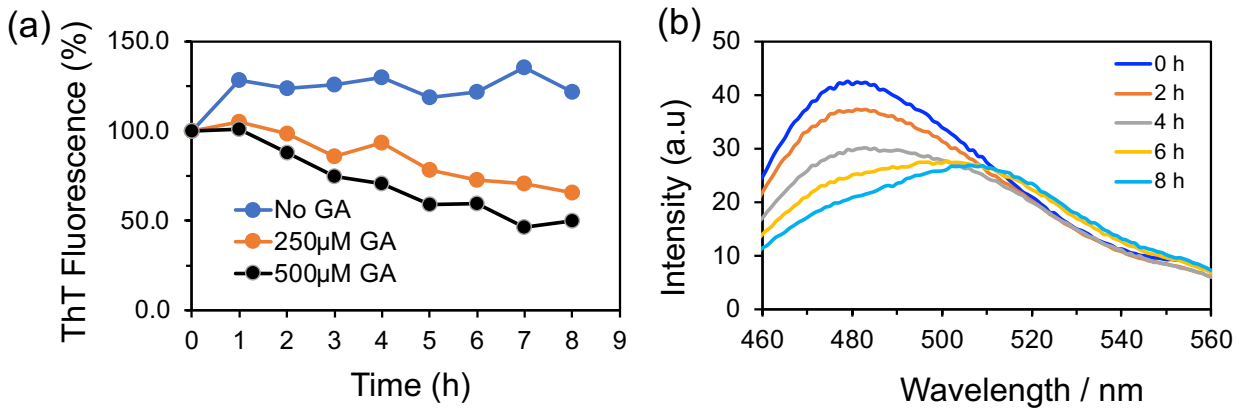

Figure S6: (a) Effect on ThT fluorescence at 480 nm upon the addition of gallic acid (250 μM and 500 μM) into **Fr-Aβ42** solution (10 μM ThT and 1μM protein) in 50 mM K-phos buffer (pH 6.8)/0.15 M NaCl. The figure represents an additional observation corresponding to Figure 4b, for the reduction of ThT fluorescence at 480 nm in pH6.8, as gallic acid oxidation is faster in alkaline pH. (b) The emission spectral traces corresponding to (a) with 250 μM of gallic acid in every 2-hour interval, demonstraing the decrease in ThT fluorescence intensity at 480 nm.

Table S1: **Fr-Aβ42** gene sequence used for expression in *E. coli*.

ATG AGC TCC CAG ATT CGT CAG AAT TAT TCT ACT GAA GTG GAG GCC GCC GTC AAC CGC CTG GTC AAC CTG TAC CTG CGG GCC TCC TAC ACC TAC CTC TCT CTG GGC TTC TAT TTC GAC CGC GAC GAT GTG GCT CTG GAG GGC GTA TGC CAC TTC TTC CGC GAG TTG GCG GAG GAG AAG CGC GAG GGT GCC GAG CGT CTC TTG AAG ATG CAA AAC CAG CGC GGC GGC CGC GCC CTC TTC CAG GAC TTG CAG AAG CCG TCC CAG GAT GAA TGG GGT ACA ACC CTG GAT GCC ATG AAA GCC GCC ATT GTC CTG GAG AAG AGC CTG AAC CAG GCC CTT TTG GAT CTG CAT GCC CTG GGT TCT GCC CAG GCA GAC CCC CAT CTC TGT GAC TTC TTG GAG AGC CAC TTC CTA GAC GAG GAG GTG AAA CTC ATC AAG AAG ATG GGC GAC CAT CTG ACC AAC ATC CAG AGG CTC GTT GGC TCC CAA GCT GGG CTG GGC GAG TAT CTC TTT GAA AGG CTC ACT CTC AAG CAC GAC GGC GGC GGC GAT GCA GAA TTC CGA CAT GAC TCA GGA TAT GAA GTT CAT CAT CAA AAA TTG GTG TTC TTT GCA GAA GAT GTG GGT TCA AAC AAA GGT GCA ATC ATT GGA CTC ATG GTG GGC GGT GTT GTC ATA GCG **TAA** *(Note: Start and stop codons are shown in bold. Black, red and blue sections represents the ferritin, GGG (linker) and $A\beta_{(1-42)}$ regions, respectively.)*

Table S2: Sequence of primers used to generate the **Fr-Aβ42** construct.

(DNA insert) 5’ -ACTCTCAAGCACGACGGCGGCGGCGATGCAGAATTCCGACATGACTCAGG -3’ (Forward) 5’- CTGCAGGTCGACTTACGCTATGACAACACCGCCCACCATGAG -3’ (Reverse)
(Vector linearization) 5’ - TAAGTCGACCTGCAGGCATGCAAGC - 3’ (Forward) 5’- GTCGTGCTTGAGAGTGAGCCTTTC -3’ (Reverse)

Table S3: Amino acid sequence in **Fr-Aβ42**.

Fr(1-174)-GGG-Aβ(1-42) >SSQIRQNYSTEVEAAVNRLVNLYLRASYTYLSLGFYFDRDDVALEGVCHFFRELAEEKREGAE RLLKMQNQRGGRALFQDLQKPSQDEWGTTLDAMKAAIVLEKSLNQALLDLHALGSAQADPHL CDFLESHFLDEEVKLIKKMGDHLTNIQRLVGSQAGLGEYLFERLTLKHDGGGDAEFRHDSGYEV HHQKLVFFAEDVGSNKGAIIGLMVGGVVIA. *(Note: Black, red and blue sections represents the ferritin, GGG (linker) and $A\beta_{(1-42)}$ regions, respectively.)*

Table S4: X-ray crystallographic data parameters and refinement statistics for **Fr-Aβ42**.

Dataset	**Fr-Aβ42**
PDB code	8KH2
Data collection	
X-ray source	Cu Kα2
Wavelength (Å)	1.541838
Data collection temperature (℃)	-180
Space group	*F*432
Cell dimension	
$a = b = c$ (Å)	181.94
$\alpha = \beta = \nu$ (°)	90.00
Resolution limit (Å)	21.69-2.0 (2.05-2.0)
Unique reflections	17564 (1264)
Multiplicity	7.4 (6.4)
Completeness (%)	97.7 (98.8)
Mean (I /sigma(I))	19.8 (6.1)
R_{merge}	0.084 (0.217)
R_{meas}	0.090 (0.237)
R_{pim}	0.033 (0.092)
Half-set correlation, CC(1/2)	0.996 (0.977)
Average mosaicity (°)	0.79
Wilson B factor (Å^2)	9.04
Refinement	
Resolution (Å)	2.00
No. reflections used	16,644
R-factor/R-free	0.216 / 0.260
No. atoms in the protein	
Amino acids	171
Assigned Cd ions	9
Water	167

***B*-factors (Å^2)**	
Overall (protein part)	14.42
Main chain	12.08
Sidechain	16.65
Waters	22.79
R.m.s. deviations from ideality	
Bond lengths (Å)	0.0134
Bond angles (°)	1.924
Ramachandran plot statics (%)	
Favored region	98.22
Allowed region	1.78
Outlier	0

Note: Values in the parentheses are for the highest-resolution shell. $R = \Sigma||F_o|-|F_c||/\Sigma|F_o|$, where F_o and F_c are the observed and calculated structure factor amplitudes, respectively. R_{free} is the R factors calculated on a partial set that is not used in the refinement of the structure.

Table S5: Selected list of reports on polypeptide fusion at the C-terminal of ferritin cage.

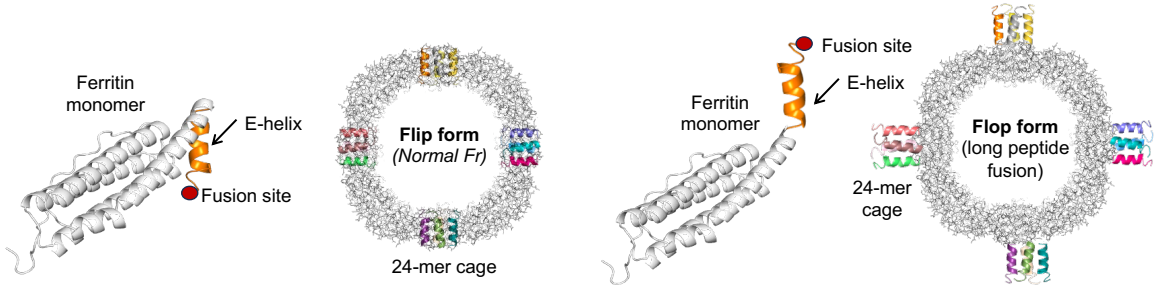

Entry	Fused peptide/protein at E-helix	No. of fused residues	Form of ferritin cage	Reference
1	Lanthanide binding tag	20	Flip form	[10]
2	Neuropilin-1 binding peptide	33	Flop form	[11]
3	ERK peptide inhibitor	34	Flop form	[12]
4	SpyTag glue peptide $(EAAAK)_{1\text{-}2}$	18-23	Flip form	[13]
	SpyTag glue peptide $(EAAAK)_{3\text{-}4}$	28-33	Flop form	[13]
	Antibody	65-68	Flop form	[13]
5	GFP	> 238	Flop form	[14]
6	Aβ peptide	45	Flip form	This work

Note. Histidine tag, Linkers, cleavage sites etc. are included in counting the total number of fused residues.

Table S6: Secondary structure analysis from CD spectra of FrWT and **Fr-Aβ42**.*

FrWT		**Fr-Aβ42**	
Before heating	**After heating**	**Before heating**	**After heating**
Helix: 100.0 %	Helix: 100.0 %	Helix: 96.0 % Antiparrel: 4.0 %	Helix: 41.5 % Antiparallel: 11.7 % Parallel: 5.8 % Turn: 7.6 % Others: 33.4 %

* The analysis was performed based on the spectra shown in Figure 5a,b using the web server: https://bestsel.elte.hu/index.php.[15] Wave length range: 190-250 nm. Scale factor: 1. Input unit: Delta epsilon.

SI References

[1] S. Thomas, N. D. Maynard and J. Gill. DNA library construction using Gibson Assembly®. *Nature Methods*, **2015**, 12, i-ii.

[2] K. Iwahori, K. Yoshizawa, M. Muraoka and I. Yamashita. Fabrication of ZnSe Nanoparticles in the Apoferritin Cavity by Designing a Slow Chemical Reaction System. *Inorg. Chem.*, **2005**, 44, 6393-6400.

[3] B. Maity and T. Ueno. A Generalized Method for Metal Fixation in Horse Spleen L-Ferritin Cage. *Methods Mol Biol*, **2023**, 2671, 135-145.

[4] P. Evans and A. McCoy. An introduction to molecular replacement. *Acta Crystallographica Section D*, **2008**, 64, 1-10.

[5] G. N. Murshudov, P. Skubak, A. A. Lebedev, N. S. Pannu, R. A. Steiner, R. A. Nicholls, M. D. Winn, F. Long and A. A. Vagin. REFMAC5 for the refinement of macromolecular crystal structures. *Acta Crystallographica Section D*, **2011**, 67, 355-367.

[6] P. Emsley, B. Lohkamp, W. G. Scott and K. Cowtan. Features and development of Coot. *Acta Crystallographica Section D*, **2010**, 66, 486-501.

[7] V. B. Chen, W. B. Arendall, III, J. J. Headd, D. A. Keedy, R. M. Immormino, G. J. Kapral, L. W. Murray, J. S. Richardson and D. C. Richardson. MolProbity: all-atom structure validation for macromolecular crystallography. *Acta Crystallographica Section D*, **2010**, 66, 12-21.

[8] B. Maity, Z. Li, K. Niwase, C. Ganser, T. Furuta, T. Uchihashi, D. Lu and T. Ueno. Single-molecule level dynamic observation of disassembly of the apo-ferritin cage in solution. *Physical Chemistry Chemical Physics*, **2020**, 22, 18562-18572.

[9] T. Ueno, K. Niwase, D. Tsubokawa, K. Kikuchi, N. Takai, T. Furuta, R. Kawano and T. Uchihashi. Dynamic behavior of an artificial protein needle contacting a membrane observed by high-speed atomic force microscopy. *Nanoscale*, **2020**, 12, 8166-8173.

[10] L. Calisti, M. C. Trabuco, A. Boffi, C. Testi, L. C. Montemiglio, A. des Georges, I. Benni, A. Ilari, B. Taciak, M. Białasek, T. Rygiel, M. Król, P. Baiocco and A. Bonamore. Engineered ferritin for lanthanide binding. *PLOS ONE*, **2018**, 13, e0201859.

[11] Y. Ma, Y. Dong, X. Li, F. Wang and Y. Zhang. Tumor-Penetrating Peptide-Functionalized Ferritin Enhances Antitumor Activity of Paclitaxel. *ACS Appl. Bio Mater.*, **2021**, 4, 2654-2663.

[12] Y. Dong, Y. Ma, X. Li, F. Wang and Y. Zhang. ERK-Peptide-Inhibitor-Modified Ferritin Enhanced the Therapeutic Effects of Paclitaxel in Cancer Cells and Spheroids. *Mol. Pharm.*, **2021**, 18, 3365-3377.

[13] H. J. Oh and Y. Jung. Active drug loading and release behaviors of fourfold channel flopped-ferritin variants. *Bull. Korean Chem. Soc.*, **2021**, 42, 1666-1671.
[14] S. Kim, G. S. Kim, J. Seo, G. Gowri Rangaswamy, I.-S. So, R.-W. Park, B.-H. Lee and I.-S. Kim. Double-Chambered Ferritin Platform: Dual-Function Payloads of Cytotoxic Peptides and Fluorescent Protein. *Biomacromolecules*, **2016**, 17, 12-19.
[15] A. Micsonai, F. Wien, É. Bulyáki, J. Kun, É. Moussong, Y.-H. Lee, Y. Goto, M. Réfrégiers and J. Kardos. BeStSel: a web server for accurate protein secondary structure prediction and fold recognition from the circular dichroism spectra. *Nucleic Acids Research*, **2018**, 46, W315-W322.